

Supporting Information for ”Long-term trends in the distribution of ocean chlorophyll”

Dongran Zhai ¹, Claudie Beaulieu ¹, Raphael Kudela ¹

¹University of California, Santa Cruz, 1156 High St, Santa Cruz, CA 95064

Contents of this file

Text S1. Additional analysis performed on the OC-CCI data product.

Text S2. Additional analysis performed on the Globcolour data product.

Text S3. Definition of regions in this study.

List of figures

Figures S1: Maps of CHL trends from 1997-2022 in the OC-CCI data product after transformation using the Hildreth-Lu procedure

Figures S2: Maps of log-transformed CHL trends from 1997-2022 using OC-CCI dataset in multiple quantile levels

Figures S3: First-order autocorrelation in the residuals of the QF test in CHL from the OC-CCI data product.

Figures S4: CHL regional trends fit in OC-CCI data product at different quantile levels

Figures S5: CHL trends from the OC-CCI data product over 1997-2022 for December, January, and February (DJF) and June, July, and August (JJA)

Figures S6: Maps of CHL trends from 1997-2022 in the GlobColour data product

Figures S7: CHL regional trends and uncertainties in GlobColour data product in different quantile levels

Figures S8: CHL regional trends fit in GlobColour data product at different quantile levels

Text S1: Additional analysis performed on the OC-CCI data product

In this section, we provide additional analysis on the OC-CCI dataset. We provide more details on pre-whitening and also include results using a different pre-whitening approach and assess whether a log-transformation affects our results. We also assess the impact of regional seasonality on trends detected in several quantiles.

S1.1 Additional details on trends and transformations

In the main text, we used the Cochrane-Orcutt transformation to remove autocorrelation before detecting trends in different CHL quantiles. Here, we use the Hildreth-Lu procedure (Figure S1) to deal with autocorrelation in the CHL time series. The magnitude of trends and significance area at a 5% level on a global scale are similar. We also include trends detected in log-transformed CHL to assess whether our results are sensitive to such a transformation (Figure S2). Trends are similar in both CHL and log-transformed CHL, and this transformation does not impact our results.

The autoregressive parameter ϕ_τ is estimated and has a similar value in two procedures (Figure S3). Note that only the 5th percent quantile level is shown, but the first-order autocorrelation level is similar in other quantiles. Additionally, Figure S4 shows the time

series of regional chlorophyll-a with regional trends in multiple quantile levels obtained with a Cochrane-Orcutt transformation.

S1.2 Impact of Regional Seasonality

To better describe the impact of seasonality on long-term trends, we apply the quantile regression analysis on the time series of averaged CHL during DJF and JJA, respectively (Figure S5). Though the results show positive trends in the 95th quantile in the high latitudes of the North Pacific and North Atlantic, the area of significant trends almost double in DJF compared to that in the JJA (Figure S5b and S5d). The trends magnify with the increase of quantiles from the 50th to 95th quantile levels in both seasonal periods. In addition, trends and variability of CHL in the Southern Ocean are increasing over time in all quantile levels, particularly in the region around Antarctica, as shown in the main text. Although CHL in the Southern Ocean reaches its maximum during the austral spring and summer, i.e. DJF, whereas the magnitude slightly decreases during the winter months, i.e. JJA, more significant trends are detected in JJA (Figure S5b and S5d). These findings suggest that trends in CHL extremes high in the north hemisphere are mainly associated with DJF, but CHL extremes high are dominated by JJA in the southern hemisphere.

Notably, trends in the upper quantile level in the eastern Equatorial Pacific region exhibit an opposite seasonal pattern compared to trends in high latitudes (Figure S5b and S5d). Although negative trends are detected in the upper quantile levels in both winter and summer time, both magnitude and area of significant trends are larger in JJA.

Text S2: Additional analysis performed on the Globcolour data product

Here, we present comprehensive quantile regression results of the GlobColour data product, including maps of chlorophyll-a trends from 1997-2022 after a Cochrane-Orcutt transformation, trends and variability in different quantile levels estimated globally (Figure S6) and regionally.

S2.1 Comparison of Two Data Products

Though positive trends in the upper quantile are larger than in the lower quantile in Subantarctic Province, the increasing variabilities of trends are consistent in all quantile levels in the two datasets (see main text and S7c). Trends in lower quantile are negative but are close to zero in most quantile levels in North Pacific Subarctic Gyres, North Pacific, and North Atlantic Subtropical Gyres (Figure S7a, S7e, and S7f). Conversely, trends in lower quantile are positive and negative in middle and upper quantile levels in North Atlantic Drift and Pacific Equatorial Province (Figure S7b and S7d). In these five regions, trends in all quantile levels are consistent with decreasing variability. Larger uncertainties are associated with low quantiles (5th and 10th), and uncertainties in the upper quantiles are far smaller and evenly with uncertainties in middle quantiles. Similarly, trend estimates obtained by the OLS model and median quantile level (50th) are overlapped, which is consistent in the two datasets (Figure S8).

Text S3: Definition of regions in this study

Regions are defined by Longhurst (1995), according to physical forcing and biogeochemical characteristics. The regions mentioned in this study are corresponding with Longhurst Province. North Pacific Subarctic Province indicates Eastern and Western Pacific subarctic gyres (PSAE and PSAW). North Atlantic Drift Province indicates North Atlantic Drift (NADR). Subantarctic Province indicates Subantarctic water ring (SANT). Pacific Equatorial Province indicates North Pacific equatorial counter current (PNEC) and Pacific equatorial divergence (PEQD). North Pacific Subtropical Gyre indicates Northwest Pacific subtropical (NPTW). North Atlantic Subtropical Gyre indicates Northwest and Northeast Atlantic subtropical gyral (NASW and NASE).

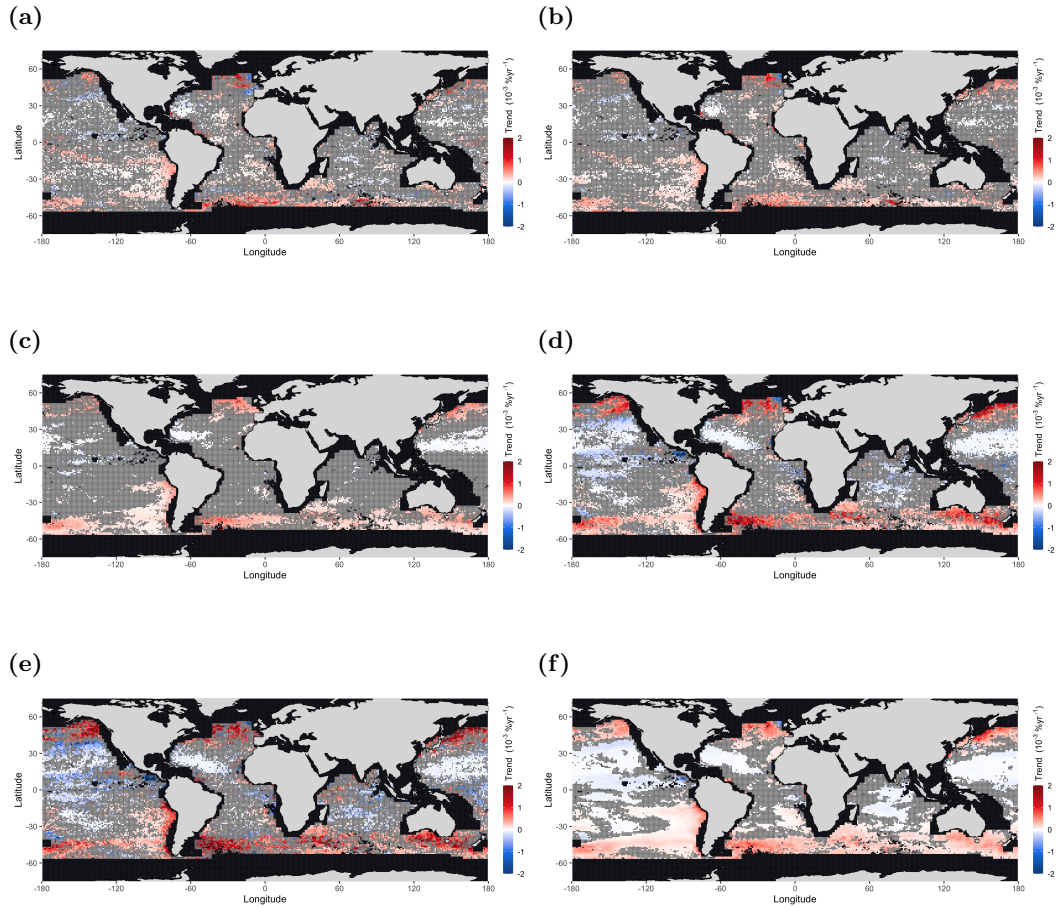


Figure S1 Maps of CHL trends from the OC-CCI data product during 1997-2022 in (a) 5th, (b) 10th, (c) 50th, (d) 90th, (e) 95th quantile levels, and (f) in CHL mean, respectively. Trends were fitted to transformed data to remove autocorrelation via the Hildreth-Lu procedure. The grey shadows are regions where trends are not significant at a 5% level.

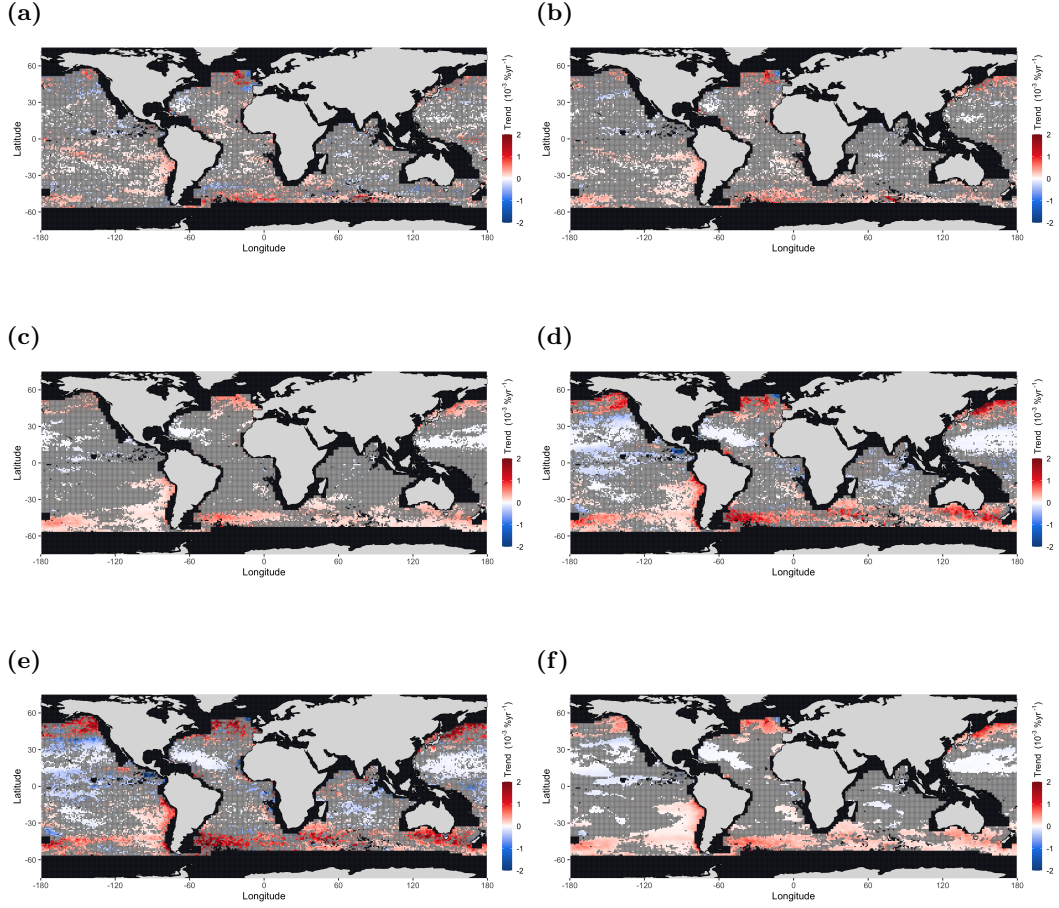


Figure S2 Maps of log-transformed CHL trends from the OC-CCI data product during 1997-2022 in (a) 5th, (b) 10th, (c) 50th, (d) 90th, (e) 95th quantile levels and (f) in CHL mean, respectively. Trends were fitted to transformed data to remove autocorrelation via the Cochrane-Orcutt procedure. The grey shadows are regions where trends are not significant at a 5% level.

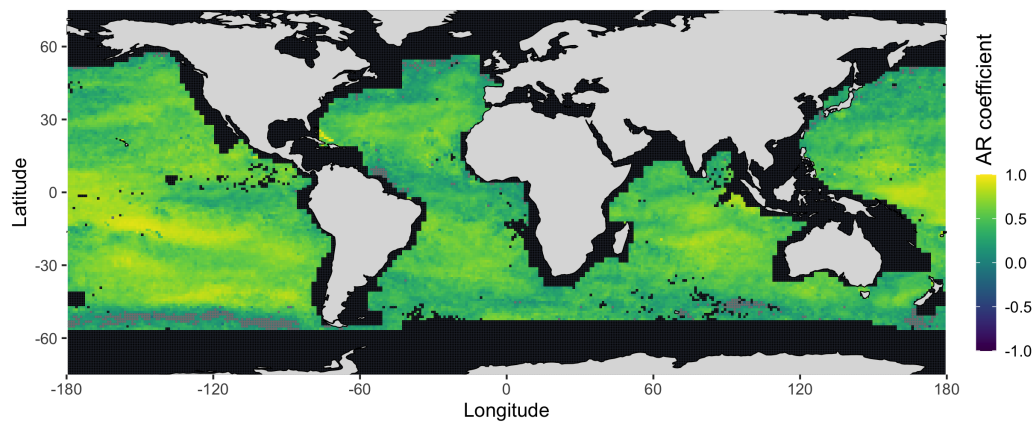


Figure S3 First-order autocorrelation in the residuals of the QF test in CHL from the OC-CCI data product. The grey shadows are regions where trends are not significant at a 5% level.

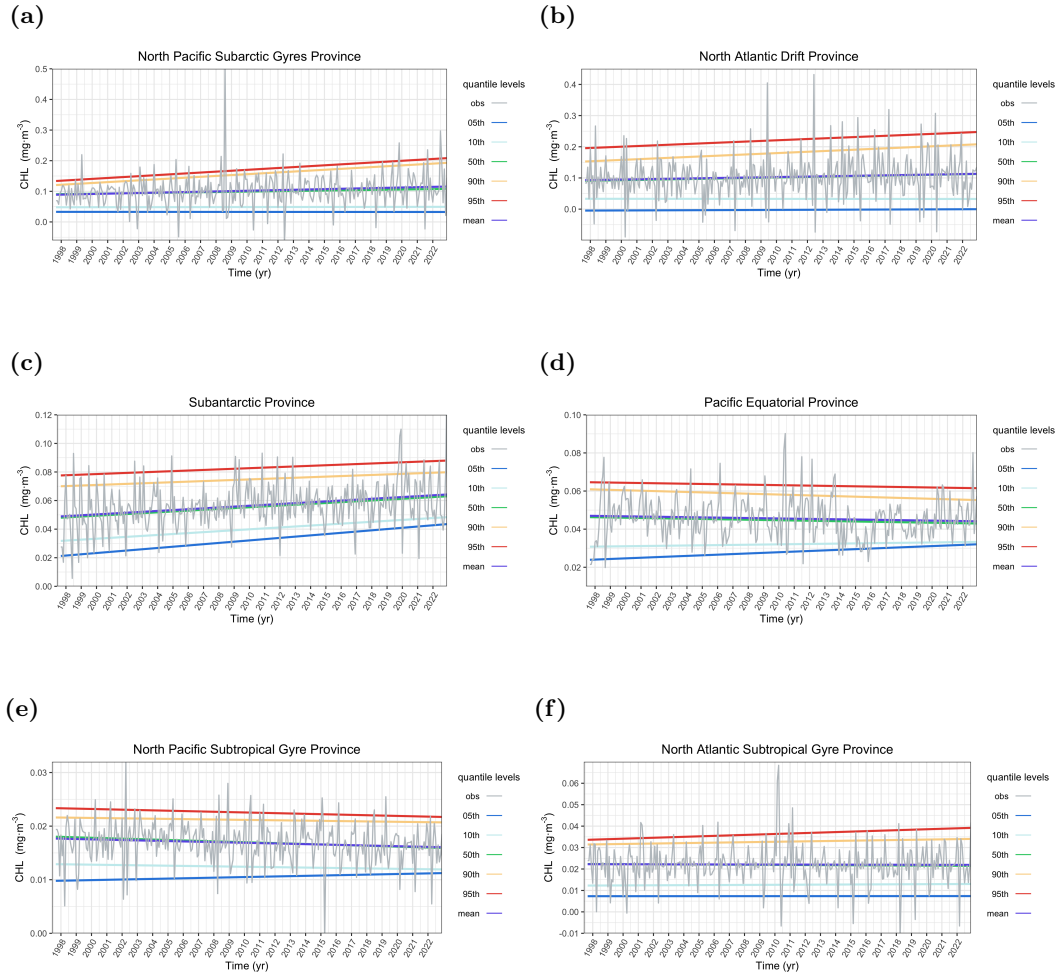


Figure S4 CHL trends in OC-CCI data product in different quantile levels in regions, namely (a) North Pacific Subarctic Gyre Province, (b) North Atlantic Drift Province, (c) Subantarctic Province, (d) Pacific Equatorial Province, (e) North Pacific Subtropical Gyre Province, and (f) North Atlantic Subtropical Gyre Province.

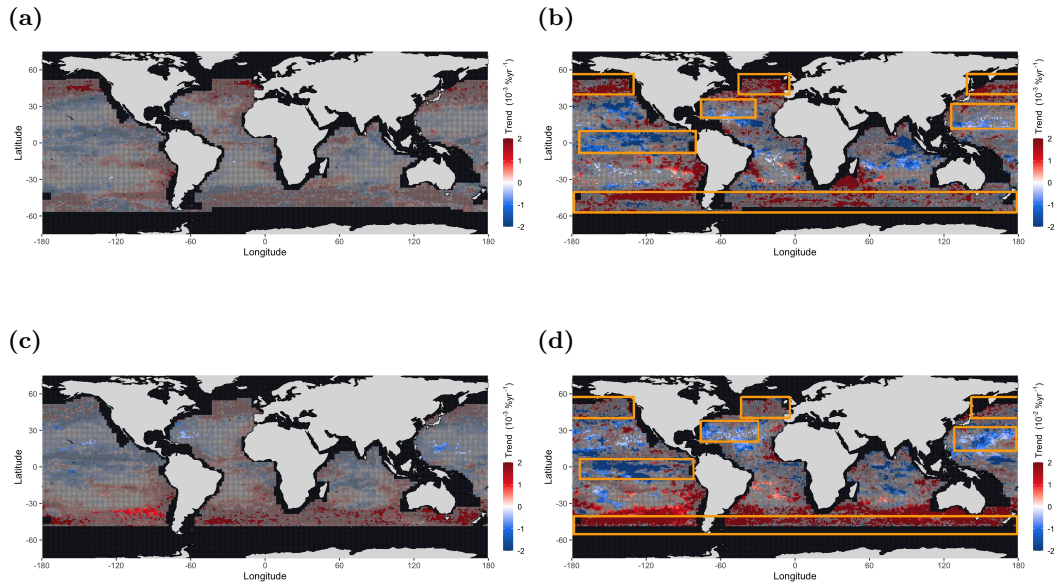


Figure S5 CHL trends from the OC-CCI data product over 1997-2022 in (a) 50th quantile level trends in December, January, and February (DJF) CHL means (b) 95th quantile level trends in DJF CHL means (c) 50th quantile level trends in June, July, and August (JJA) CHL means, and (d) 95th quantile level trends in JJA CHL means. The orange boxes are regions of interest with trends significant in multiple quantiles. The overlapped stippling shows areas where the trends are not significant at a 5% level.

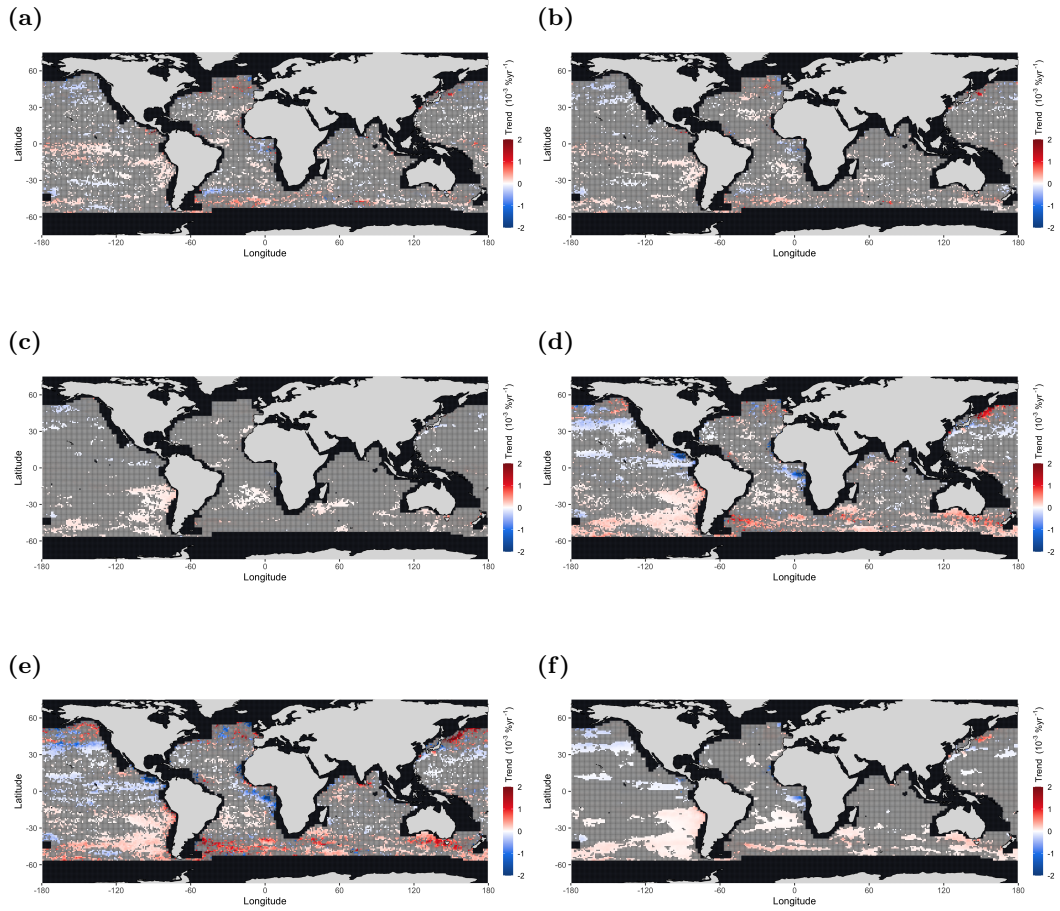


Figure S6 Maps of CHL trends from the GlobColour data product during 1997-2022 in (a) 5th, (b) 10th, (c) 50th, (d) 90th, (e) 95th quantile levels, and (f) in CHL mean, respectively. Trends were fitted to transformed data to remove autocorrelation via the Cochrane-Orcutt procedure. The grey shadows are regions where trends are not significant at a 5% level.

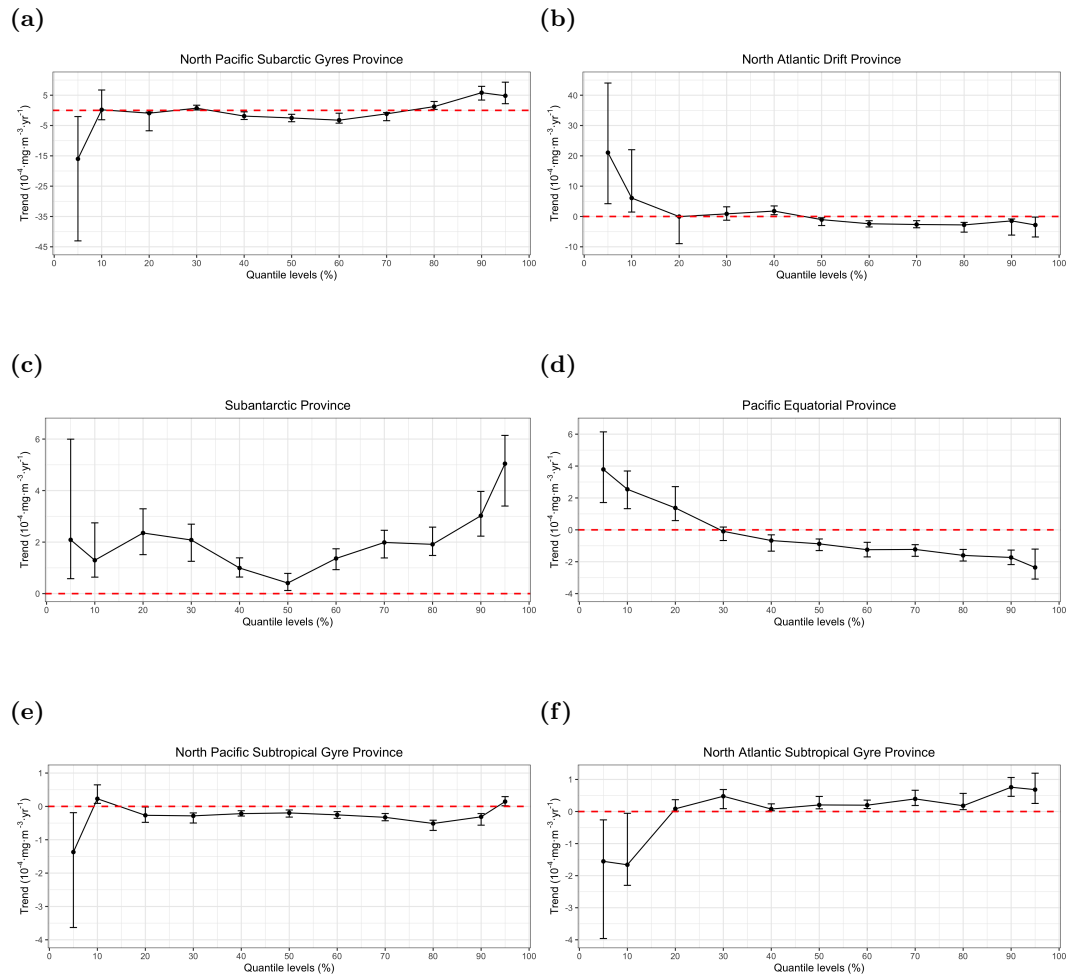


Figure S7 Regional CHL trends in GlobColour data product in different quantile levels in regions, (a) North Pacific Subarctic Gyre Province, (b) North Atlantic Drift Province, (c) Subantarctic Province, (d) Pacific Equatorial Province, (e) North Pacific Subtropical Gyre Province, and (f) North Atlantic Subtropical Gyre Province. The 95% confidence intervals for each regression are represented by the vertical lines. The red horizontal dashed line is zero.

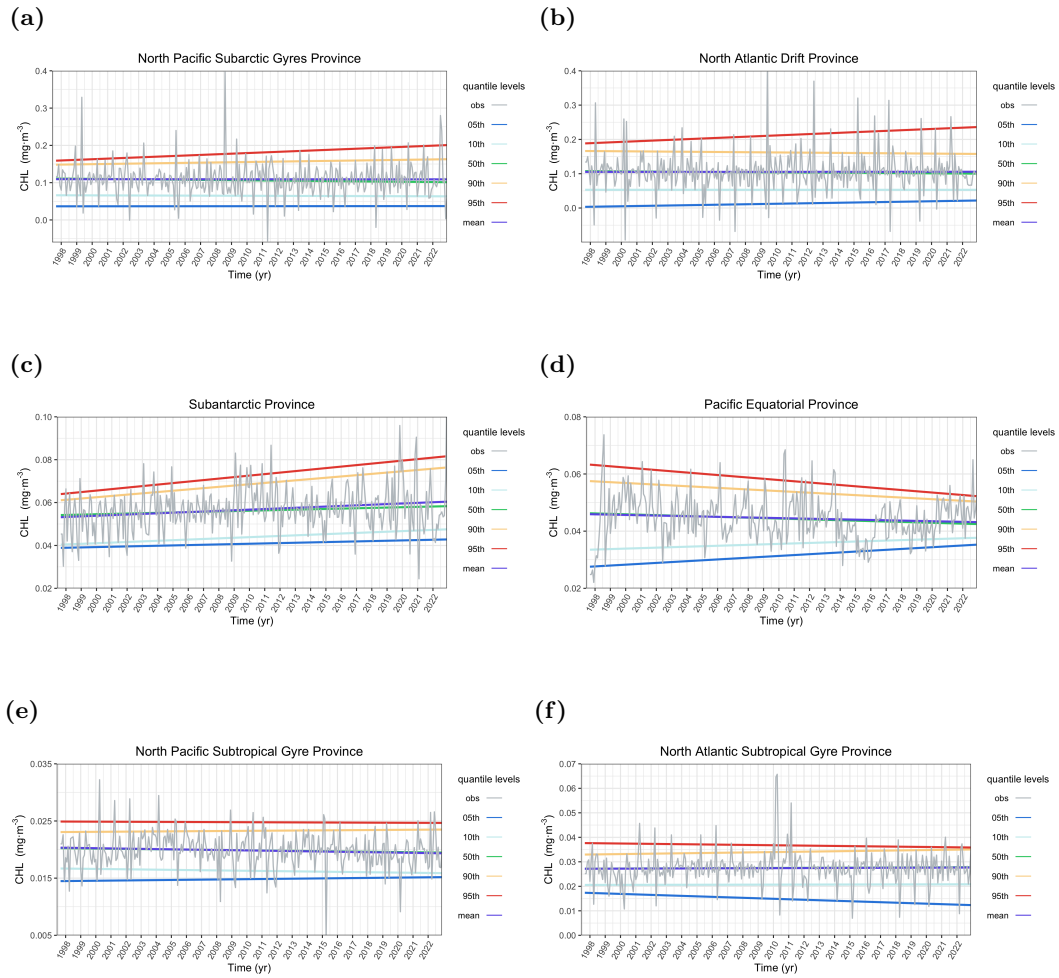


Figure S8 CHL trends in GlobColour data product in different quantile levels in regions, namely (a) North Pacific Subarctic Gyre Province, (b) North Atlantic Drift Province, (c) Subantarctic Province, (d) Pacific Equatorial Province, (e) North Pacific Subtropical Gyre Province, and (f) North Atlantic Subtropical Gyre Province.